GMR Genetics and Molecular Research
Online Journal
ISSN:1676-5680

Integrated miRNA-mRNA analysis of Epstein-Barr virus-positive nasopharyngeal carcinoma

L.H. Zhu[1]*, X.T. Miao[2]* and N.Y. Wang[3]

[1]Department of Otolaryngology & Head and Neck Surgery, Beijing Chaoyang Hospital, Capital Medical University, Shijingshan District, Beijing, China
[2]Department of Otolaryngology & Head and Neck Surgery, Beijing Jishuitan Hospital, XiCheng District, Beijing, China
[3]Department of Otolaryngology & Head and Neck Surgery, Beijing Chaoyang Hospital, Capital Medical University, Chaoyang District, Beijing, China

*These authors contributed equally to this study.
Corresponding author: N.Y. Wang
E-mail: wangningyyoo@163.com

Genet. Mol. Res. 14 (2): 6028-6036 (2015)
Received September 30, 2014
Accepted February 5, 2015
Published June 1, 2015
DOI http://dx.doi.org/10.4238/2015.June.1.20

ABSTRACT. This study aims to identify the crucial miRNAs in Epstein-Barr virus-positive nasopharyngeal carcinoma (NPC) and their target genes. Gene expression profile data (GSE12452) that included 31 NPC and 10 normal nasopharyngeal tissue specimens were downloaded. Differentially expressed genes (DEGs) were identified using significance analysis of microarrays. The underlying function of DEGs was predicted via Gene Ontology and Kyoto Encyclopedia of Genes and Genomes pathway enrichment analyses. The miRNA sequencing dataset GSE14738 was also downloaded, and expression levels of miRNA were calculated by the number of reads mapped to each miRNA. The selected miRNAs were integrated into the miRecords

database to obtain their target genes. Target genes associated with DEGs were used to construct the interaction network via Cytoscape. A total of 1437 DEGs between NPC and control were identified, most of which were enriched in cell cycle and extracellular matrix-receptor interaction signaling pathways. Furthermore, 112 miRNAs were considered upregulated in NPC samples. A total of 2228 relationships between 39 miRNAs and 1247 target genes were obtained, of which 182 relationships between 32 miRNAs and 97 target genes were chosen to construct an interaction network. The interactions between DEGs and the let-7 or miR-29 families appeared strongest in this network, where *CDC25A*, *COL3A1*, and *COL1A1* were regulated by several let-7 family members, while *COL4A1* and *COL5A2* were regulated by several miR-29 family members. The let-7 and miR-29 families may be related to the development of NPC by regulating the genes involved in cell cycle and ECM-receptor interaction.

Key words: Epstein-Barr virus-positive nasopharyngeal carcinoma; Differentially expressed genes; Typical miRNAs; Target genes

INTRODUCTION

Nasopharyngeal carcinoma (NPC), an epithelial malignancy of the nasopharynx, frequently occurs in southern China and Southeast Asia, where incidence rates exceed 30 per 100,000 persons. NPC rates are less in the United States and other nations, with the incidence rate of only one per 100,000 persons (Chang and Adami, 2006). Epstein-Barr virus (EBV) infection is commonly linked to the development of NPC. Constitutive expression of the latent membrane protein-1 of EBV can activate nuclear factor kappa B, Janus tyrosine kinase/signal transducers and activators of transcription, and c-jun N-terminal kinase/activator protein 1 signaling pathways and induce the transcription of several oncogenic factors that ultimately promote cancerous phenotypes including proliferation, migration, invasion, and metastasis (Yu et al., 2013; Zhao et al., 2014). Thus, targeting the virus through approaches such as EBV-specific antibodies and viral lytic induction are recommended for treating NPC (Hutajulu et al., 2014; Coghill and Hildesheim, 2014). However, not all tumor tissues express viral oncoproteins, suggesting that other mechanisms may lead to the aggressive behavior of NPC tumor cells.

Recently, more studies have attempted to investigate whether miRNAs play a role in NPC initiation, promotion, and progression by regulating their target genes. For example, Cheung et al. (2014) reported that miR-31 suppressed NPC cell growth by targeting factor inhibiting hypoxia-inducible factor 1-alpha and minichromosome maintenance proteins 2. Lyu et al. (2014) demonstrated that miR-93 can attenuate Smad-dependent transforming growth factor-β (TGF-β) signaling and activate the phosphatidylinositol 3-kinase/protein kinase B pathway by inhibiting the TGF-β receptor II, further promoting the uncontrolled growth, invasion, metastasis, and epithelial-to-mesenchymal transition-like process of NPC cells. However, the pathogenesis of NPC remains unclear. In the present study, we aimed to further identify crucial miRNAs and their target genes utilizing the gene expression profile data of GSE12452 (Dodd et al., 2006; Sengupta et al., 2006; Hsu et al., 2012) and the miRNA sequencing dataset

GSE14738 (Zhu et al., 2009). Candidate target genes identified by multi-bioinformatic methods may provide the groundwork for a combination therapy approach for EBV-positive NPC.

MATERIAL AND METHODS

Affymetrix microarray data and preprocessing

The gene expression profile data GSE12452 (Dodd et al., 2006; Sengupta et al., 2006; Hsu et al., 2012) were downloaded from Gene Expression Omnibus (GEO) database (http://www.ncbi.nlm.nih.gov/geo/), which included 31 EBV-positive NPCs and 10 normal nasopharyngeal tissue specimens. The annotation information for the chip was downloaded from the Human Genome U133 Plus 2.0 Array (Affymetrix, Santa Clara, CA, USA GPL570 platform). The original probe-level data in CEL files were converted into expression measures by Affypackage (Gautier et al., 2004) in Bioconductor of R language (http://www.R-project.org) and were normalized by using the Robust Multi-array Average method (Irizarry et al., 2003). When multiple probes were present for a particular gene, the average expression value of those probes was used for that gene.

miRNA data and preprocessing

The miRNA high-throughput sequencing dataset GSE14738 (Zhu et al., 2009) was downloaded from Sequence Read Archive (SRA) database (http://www.ncbi.nlm.nih.gov/sra/), including 2 EBV-positive NPCs and 2 normal nasopharyngeal tissue specimens. The platform was GS20 (454 Genome Sequencer, Roche Applied Science, Indianapolis, IN, USA). The raw SRA data were converted into fast-q format. Next, base-calling was performed via the Phred/Phrap/PolyPhred 5.04 software (http://droog.mbt.washington.edu/PolyPhred.html) (Ledergerber and Dessimoz, 2011). After quality checks, the adapter and poly-A tail were cut off. Only reads with more than 15 bp were chosen for further analysis. These reads were mapped to miRBase V.20 (http://www.mirbase.org/) and were annotated by using BLAST (Kim et al., 2006). Reads mapped to mature miRNA were saved. The expression level of a particular miRNA was defined according to the number of reads mapped to it.

Identification of differentially expressed genes and miRNAs

For the gene expression profile, differentially expressed genes (DEGs) were selected using the significance analysis for microarray (SAM) method (http://www-stat.stanford.edu/~tibs/SAM/index.htlm) (Bochkis et al., 2012) in R language with the cut-off criteria of delta = 2, fold-change $\geq$ 1.5 and false discovery rate < 5%. For miRNA profiling, differentially expressed miRNAs were identified according to the number of reads mapped to this miRNA.

Functional enrichment analysis of DEGs

The screened DEGs were hierarchically clustered by Cluster in R language (Eisen et al., 1998) in order to distinguish NPC from normal nasopharyngeal tissues. The underlying function of DEGs was predicted by the Gene Ontology (GO) (Hulsegge et al., 2009) function and Kyoto Encyclopedia of Genes and Genomes (KEGG) (Kanehisa, 2002) pathway en-

richment analysis using the Database for Annotation, Visualization, and Integrated Discovery (DAVID) tool (http://www.david.niaid.nih.gov) (Huang et al., 2009). P value < 0.01 was set as the cut-off criterion.

Target genes of miRNAs

To obtain the target genes of miRNAs, the selected miRNAs were integrated into the miRecords database (http://miRecords.umn.edu/miRecords) (Xiao et al., 2009), in which the relationship between target genes and miRNAs had been confirmed. The target genes were calculated via more than 6 algorithms (total 11 algorithms). Only target genes related to the DEGs were used to construct the interaction network via Cytoscape (http://cytoscape.org) (Shannon et al., 2003).

RESULTS

Identification of DEGs

After normalization of the raw microarray data (Figure 1), 41,293 probes corresponding to 19,944 genes were obtained from 31 NPC and 10 normal healthy nasopharyngeal tissue specimens. By using the SAM algorithm, a total of 1437 DEGs were identified in NPC compared to normal nasopharyngeal tissues samples, including 619 upregulated and 818 downregulated genes. Cluster analysis of DEGs showed significant differences between NPC samples and normal nasopharyngeal tissue (Figure 2).

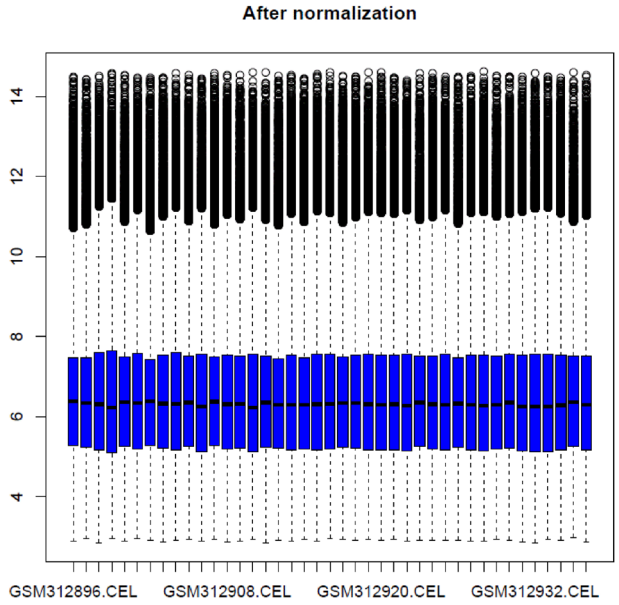

Figure 1. Boxplot of gene expression level after normalization. The horizontal axis represents samples, and the vertical axis represents gene expression level. The black line is the median of the gene expression level from each sample. The dotted line is almost a straight line, indicating that the degree of standardization was optimal.

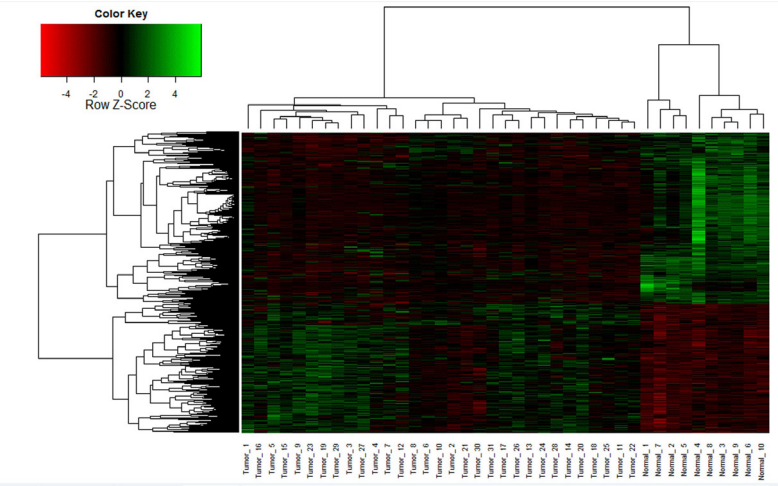

Figure 2. Cluster analyses of differentially expressed genes (DEGs). The abscissa represents different samples; the vertical axis represents clusters of DEGs. Red color represents downregulation; green color represents upregulation. Expression data are represented as normalized values (Z-scores).

Functional enrichment analysis of the DEGs

To investigate the potential function of DEGs in the development of NPC, we used the DAVID to identify over-represented GO terms and KEGG pathway at P value < 0.01. The up-regulated DEGs (e.g. *CDC25A*) were significantly enriched into 40 GO terms, including cell cycle and cell division (Table 1). However, the downregulated DEGs (e.g. *TUBB2A*) were only significantly enriched into 3 GO terms, including microtubule-based movement, microtubule-based process, and epithelial cell differentiation (Table 1). For KEGG pathway enrichment analysis, the upregulated DEGs were significantly enriched into cell cycle (e.g. *CDC25A* and *MYC*), extracellular matrix (ECM)-receptor interaction (e.g., *COL3A1*, *COL1A1*, *COL4A1*, and *COL5A2*), as well as p53 signaling pathway (e.g. *CCNG1*) (Table 2). However, the down-regulated DEGs were not significantly enriched into any pathway at P value < 0.01.

Table 1. GO function enrichment analysis of differentially expressed genes between nasopharyngeal carcinoma and normal nasopharyngeal samples.

Genes	GO_Term	Gene_num	FDR
Upregulated	GO:0007049 cell cycle	113	4.5821E-37
	GO:0022402 cell cycle process	96	2.5510E-36
	GO:0000278 mitotic cell cycle	78	2.1547E-35
	GO:0022403 cell cycle phase	82	2.4634E-35
	GO:0000279 M phase	73	2.1076E-34
	GO:0000087 M phase of mitotic cell cycle	60	2.0105E-32
	GO:0007067 mitosis	59	7.5435E-32
	GO:0000280 nuclear division	59	7.5435E-32
	GO:0048285 organelle fission	60	7.7347E-32
	GO:0051301 cell division	63	4.0562E-28
Downregulated	GO:0007018 microtubule-based movement	18	0.0002
	GO:0007017 microtubule-based process	26	0.0011
	GO:0030855 epithelial cell differentiation	18	0.0032

GO = gene ontology; FDR = false discovery rate; Gene_num = the number of enriched differentially expressed genes.

Table 2. KEGG pathway enrichment analysis ofdifferentially expressed genes between nasopharyngeal carcinoma and normal nasopharyngeal samples.

KEGG pathway	Enriched genes	FDR value
hsa04110: Cell cycle	*E2F3*, *DBF4*, *TTK*, *PRKDC*, *CHEK1*, *PTTG1*, *CHEK2*, *CCNE2*, *CDC45*, *RAD21*, *MCM7*, *CCNA2*, *MYC*, *CDC7*, *CDC6*, *CDK1*, *MCM2*, *CDK4*, *MCM3*, *MCM4*, *CDC25A*, *MCM6*, *CCNB1*, *YWHAG*, *MAD2L1*, *CCND2*, *PCNA*, *BUB1B*	2.22E-10
hsa03030: DNA replication	*POLA1*, *MCM2*, *MCM3*, *RNASEH2A*, *MCM4*, *MCM6*, *RFC5*, *PRIM1*, *DNA2*, *RFC3*, *RFC4*, *MCM7*, *POLE2*, *PCNA*, *FEN1*	3.44E-08
hsa04512: ECM-receptor interaction	*COL4A2*, *COL4A1*, *COL3A1*, *ITGA1*, *COL5A2*, *COL5A1*, *SDC2*, *HMMR*, *ITGAV*, *COL6A3*, *COL1A2*, *LAMC1*, *COL1A1*, *LAMB1*, *THBS2*, *FN1*	0.0009
hsa04115: p53 signaling pathway	*BID*, *CDK1*, *CYCS*, *CHEK1*, *CHEK2*, *PMAIP1*, *CCNG1*, *CDK4*, *CCNB1*, *CCNE2*, *CCND2*, *RRM2*, *FAS*	0.0140

KEGG = Kyoto Encyclopedia of Genes and Genomes; FDR = false discovery rate; ECM = extracellular matrix.

Identification of highly expressed miRNAs

The number of reads of 264 miRNAs in NPC samples was larger than that of the normal nasopharyngeal tissues. Furthermore, the miRNAs with the number of reads > 3 in two NPC samples compared with the normal nasopharyngeal tissues were selected as being highly expressed; this included 112 miRNAs.

Prediction of miRNA-targeted genes

A total of 39 miRNAs and 1247 target genes associated with EBV-positive NPC were selected from the miRecords database. A total of 2228 relationships between miRNAs and target genes were identified, of which 182 relationships (32 miRNAs and 97 target genes) were chosen to construct the interaction network (Figure 3). From the interaction network, we observed that the interactions between DEGs and the let-7 or miR-29 families were the strongest; the DEGs were regulated by several let-7 (e.g. *CDC25A*, *COL3A1*, and *COL1A1*) or miR-29 (e.g. *COL4A1* and *COL5A2*) family members. Moreover, the targets of let-7 and miR-29 families were always significantly upregulated, but the target genes of other miRNAs were upregulated or downregulated.

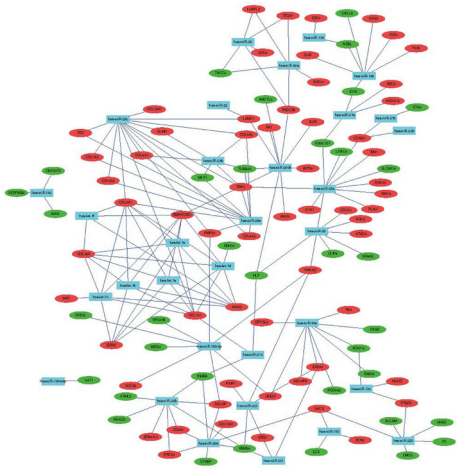

Figure 3. Interaction network of miRNAs and target genes. Blue boxes represent upregulated miRNAs; green ovals represent downregulated target genes of miRNAs; and red ovals represent upregulated target genes of miRNAs.

DISCUSSION

Based on the gene expression profiles and miRNA sequencing data, 97 DEGs were found to be regulated by 32 miRNAs and were found to participate in the development of EBV-positive NPC. Furthermore, we found that the target genes of these miRNAs might promote cancer progression by regulating the cell cycle (e.g. *CDC25A* and *MYC*) and ECM-receptor interaction (e.g. *COL3A1*, *COL1A1*, *COL4A1*, *COL5A2*).

CDC25A is an essential phosphatase for cell-cycle progression from the G1 to the S phase and acts by dephosphorylating and activating the cyclin-dependent kinase complexes. *CDC25A* mRNA was found to be highly expressed in some cancers and was correlated with more aggressive stages and poor prognosis (Boutros et al., 2007). Inhibition of *CDC25A* leads to the impairment of cell proliferation and induction of cell apoptosis, thus preventing cancer cell metastasis (Feng et al., 2011; Tu et al., 2011; Bana et al., 2013). Furthermore, some studies have demonstrated that *CDC25A* expression in cancer cells can be regulated by miR-21 (Jin et al., 2011) and miR-365 (Guo et al., 2013). In this study, we found that high *CDC25A* expression in NPC may be modulated by let-7; this has not been reported previously.

MYC is another critical gene in modulating cell cycle progression, apoptosis, and cellular transformation. As a transcription factor, *c-Myc* has been shown to promote the transcription of B-lymphoma mouse Moloney leukemia virus insertion region 1 (*Bmi-1*) in NPC by binding the E-box element (-181) within its promoter (Wang et al., 2013), while overexpression of Bmi-1 reduces the expression of p16 (INK4a), a cyclin-dependent kinase inhibitor 2A, and induces epithelial-to-mesenchymal transition in human nasopharyngeal epithelial cells, promoting NPC progression (Song et al., 2009; Wu et al., 2011). In addition, Zhou et al. (2013) also reported that *c-Myc* could directly bind to the promoter region of branched-chain amino acid transaminase 1 and upregulate its expression, followed by the increased proliferation, migration, and invasion of NPC cells. Furthermore, a recent study suggests that miR-184 mediates the direct suppression of *MYC*, thus repressing the cell proliferation and survival in NPC (Zhen et al., 2013). By gene-miRNA network analysis, we found that upregulated *MYC* expression may be mediated by let-7c, indicating an important role for let-7c in development; this was consistent with the previous study (Nadiminty et al., 2012).

COL3A1, *COL1A1*, *COL4A1*, and *COL5A2* encode collagen, an important ECM structural protein secreted by a variety of stromal cells. Collagen crosslinking triggers tumor matrix stiffening and leads to enhanced integrin clusters that in turn phosphorylate focal adhesion kinase and activate the AKT, ERK, and Rho pathways (Ng and Brugge, 2009). These pathways can control cell migration, invasion, and proliferation, leading to tumor progression (Provenzano et al., 2009). *COL3A1*, *COL1A1*, *COL4A1*, and *COL5A2* have been found in many cancers and are markers for poor prognosis (Fischer et al., 2001; Hayashi et al., 2014; Xiong et al., 2014). Furthermore, *COL3A1* is validated as a functional direct target gene of let-7d *in vitro* and *in vivo*, and COL3A1 expression was found to be inversely correlated with let-7d levels in renal cell carcinoma specimens (Su et al., 2014); a relationship also confirmed in our study. Meanwhile, we also found that *COL3A1*, *COL1A1*, *COL4A1*, and *COL5A2* might be targets of miR-29 in NPC. This observation invites further investigation.

In conclusion, our findings indicate that *CDC25A*, *MYC*, *COL3A1*, *COL1A1*, *COL4A1*, and *COL5A2* may be important targets for the treatment of NPC. Further studies are essential for confirming the regulatory relationship between these genes and their regulators, let-7 and miR-29.

REFERENCES

Bana E, Sibille E, Valente S, Cerella C, et al. (2013). A novel coumarin-quinone derivative SV37 inhibits CDC25 phosphatases, impairs proliferation, and induces cell death. *Mol. Carcinog*. 54: 229-241.

Bochkis IM, Schug J, De DY, Kurinna S, et al. (2012). Genome-wide location analysis reveals distinct transcriptional circuitry by paralogous regulators Foxa1 and Foxa2. *PLoS Genet.* 8: e1002770.

Boutros R, Lobjois V and Ducommun B (2007). CDC25 phosphatases in cancer cells: key players? Good targets? *Nat. Rev. Cancer* 7: 495-507.

Chang ET and Adami HO (2006). The enigmatic epidemiology of nasopharyngeal carcinoma. *Cancer Epidemiol. Biomarkers Prev*. 15: 1765-1777.

Cheung CC, Chung GT, Lun SW, To KF, et al. (2014). *miR-31* is consistently inactivated in EBV-associated nasopharyngeal carcinoma and contributes to its tumorigenesis. *Mol. Cancer* 13: 184.

Coghill AE and Hildesheim A (2014). Epstein-barr virus antibodies and the risk of associated malignancies: review of the literature. *Am. J. Epidemiol*. 187: 687-695.

Dodd LE, Sengupta S, Chen I-H, den Boon JA, et al. (2006). Genes involved in DNA repair and nitrosamine metabolism and those located on chromosome 14q32 are dysregulated in nasopharyngeal carcinoma. *Cancer Epidemiol. Biomarkers Prev*. 15: 2216-2225.

Eisen MB, Spellman PT, Brown PO and Botstein D (1998). Cluster analysis and display of genome-wide expression patterns. *Proc. Natl. Acad. Sci*. 95: 14863-14868.

Feng X, Wu Z, Wu Y, Hankey W, et al. (2011). Cdc25A regulates matrix metalloprotease 1 through Foxo1 and mediates metastasis of breast cancer cells. *Mol. Cell Biol*. 31: 3457-3471.

Fischer H, Stenling R, Rubio C and Lindblom A (2001). Colorectal carcinogenesis is associated with stromal expression of COL11A1 and COL5A2. *Carcinogenesis* 22: 875-878.

Gautier L, Cope L, Bolstad BM and Irizarry RA (2004). Affy-analysis of Affymetrix GeneChip data at the probe level. *Bioinformatics* 20: 307-315.

Guo SL, Ye H, Teng Y, Wang YL, et al. (2013). Akt-p53-miR-365-cyclin D1/cdc25A axis contributes to gastric tumorigenesis induced by PTEN deficiency. *Nat. Commun*. 4: 2544.

Hayashi M, Nomoto S, Hishida M, Inokawa Y, et al. (2014). Identification of the collagen type 1 alpha 1 gene (COL1A1) as a candidate survival-related factor associated with hepatocellular carcinoma. *BMC Cancer* 14: 108.

Hsu WL, Tse KP, Liang S, Chien YC, et al. (2012). Evaluation of human leukocyte antigen-A (HLA-A), other non-HLA markers on chromosome 6p21 and risk of nasopharyngeal carcinoma. *PloS One* 7: e42767.

Huang DW, Sherman BT and Lempicki RA (2009). Systematic and integrative analysis of large gene lists using DAVID bioinformatics resources. *Nature Protoc*. 4: 44-57.

Hulsegge I, Kommadath A and Smits MA (2009). Globaltest and GOEAST: Two different approaches for gene ontology analysis. *BMC Proc*. 3 (Supp 4): S10.

Hutajulu SH, Kurnianda J, Tan IB and Middeldorp JM (2014). Therapeutic implications of Epstein-Barr virus infection for the treatment of nasopharyngeal carcinoma. *Ther. Clin. Risk Manag*. 10: 721-736.

Irizarry RA, Hobbs B, Collin F, Beazer-Barclay YD, et al. (2003). Exploration, normalization, and summaries of high density oligonucleotide array probe level data. *Biostatistics* 4: 249-264.

Jin Y (2011). 3,3'-Diindolylmethane inhibits breast cancer cell growth via miR-21-mediated Cdc25A degradation. *Mol. Cell Biochem*. 358: 345-354.

Kanehisa M (2002). The KEGG database. *Novartis Found. Symp*. 247: 91-101.

Kim HJ, Cui XS, Kim EJ, Kim WJ, et al. (2006). New porcine microRNA genes found by homology search. *Genome* 49: 1283-1286.

Ledergerber C and Dessimoz C (2011). Base-calling for next-generation sequencing platforms. *Brief. Bioinform*. 12: 489-497.

Lyu X, Fang W, Cai L, Zheng H, et al. (2014). TGFbetaR2 is a major target of miR-93 in nasopharyngeal carcinoma aggressiveness. *Mol. Cancer* 13: 51.

Nadiminty N, Tummala R, Lou W, Zhu Y, et al. (2012). MicroRNA let-7c is downregulated in prostate cancer and suppresses prostate cancer growth. *PloS One* 7: e32832.

Ng MR and Brugge JS (2009). A stiff blow from the stroma: collagen crosslinking drives tumor progression. *Cancer Cell* 16: 455-457.

Provenzano PP, Inman DR, Eliceiri KW and Keely PJ (2009). Matrix density-induced mechanoregulation of breast cell phenotype, signaling and gene expression through a FAK-ERK linkage. *Oncogene* 28: 4326-4343.

Sengupta S, den Boon JA, Chen IH, Newton MA, et al. (2006). Genome-wide expression profiling reveals EBV-associated inhibition of MHC class I expression in nasopharyngeal carcinoma. *Cancer Res*. 66: 7999-8006.

Shannon P, Markiel A, Ozier O, Baliga NS, et al. (2003). Cytoscape: a software environment for integrated models of biomolecular interaction networks. *Genome Res*. 13: 2498-2504.

Song LB, Li J, Liao WT, Feng Y, et al. (2009). The polycomb group protein Bmi-1 represses the tumor suppressor PTEN and induces epithelial-mesenchymal transition in human nasopharyngeal epithelial cells. *J. Clin. Invest*. 119: 3626-3636.

Su B, Zhao W, Shi B, Zhang Z, et al. (2014). Let-7d suppresses growth, metastasis, and tumor macrophage infiltration in renal cell carcinoma by targeting COL3A1 and CCL7. *Mol. Cancer* 13: 206.

Tu YS, Kang XL, Zhou JG, Lv XF, et al. (2011). Involvement of Chk1-Cdc25A-cyclin A/CDK2 pathway in simvastatin induced S-phase cell cycle arrest and apoptosis in multiple myeloma cells. *Eur. J. Pharmacol*. 670: 356-364.

Wang HB, Liu GH, Zhang H, Xing S, et al. (2013). Sp1 and c-Myc regulate transcription of BMI1 in nasopharyngeal carcinoma. *FEBS J*. 280: 2929-2944.

Wu J, Hu D, Yang G, Zhou J, et al. (2011). Down-regulation of BMI-1 cooperates with artemisinin on growth inhibition of nasopharyngeal carcinoma cells. *J. Cell Biochem*. 112: 1938-1948.

Xiao F, Zuo Z, Cai G, Kang S, et al. (2009). miRecords: an integrated resource for microRNA-target interactions. *Nucleic Acids Res*. 37: D105-D110.

Xiong G, Deng L, Zhu J, Rychahou PG, et al. (2014). Prolyl-4-hydroxylase alpha subunit 2 promotes breast cancer progression and metastasis by regulating collagen deposition. *BMC Cancer* 14: 1.

Yu PH, Chou SF, Chen CL, Hung H, et al. (2013). Upregulation of endocan by Epstein-Barr virus latent membrane protein 1 and its clinical significance in nasopharyngeal carcinoma. *PLoS One* 8: e82254.

Zhao Y, Pang TY, Wang Y, Wang S, et al. (2014). LMP1 stimulates the transcription of eIF4E to promote the proliferation, migration and invasion of human nasopharyngeal carcinoma. *FEBS J*. 281: 3004-3018.

Zhen Y, Liu Z, Yang H, Yu X, et al. (2013). Tumor suppressor PDCD4 modulates miR-184-mediated direct suppression of C-MYC and BCL2 blocking cell growth and survival in nasopharyngeal carcinoma. *Cell Death Dis*. 4: e872.

Zhou W, Feng X, Ren C, Jiang X, et al. (2013). Over-expression of BCAT1, a c-Myc target gene, induces cell proliferation, migration and invasion in nasopharyngeal carcinoma. *Mol. Cancer* 12: 53.

Zhu JY, Pfuhl T, Motsch N, Barth S, et al. (2009). Identification of novel Epstein-Barr virus microRNA genes from nasopharyngeal carcinomas. *J. Virol*. 83: 3333-3341